Temporal Variations in Global Seismic Station Ambient Noise Power Levels

A. T. Ringler, L. S. Gee, and C. R. Hutt

U.S. Geological Survey, Albuquerque Seismological Laboratory

D. E. McNamara

U.S. Geological Survey, National Earthquake Information Center

INTRODUCTION

Recent concerns about time-dependent response changes in broadband seismometers have motivated the need for methods to monitor sensor health at Global Seismographic Network (GSN) stations. We present two new methods for monitoring temporal changes in data quality and instrument response transfer functions that are independent of Earth seismic velocity and attenuation models by comparing power levels against different baseline values.

Our methods can resolve changes in both horizontal and vertical components in a broad range of periods (~0.05 to 1,000 seconds) in near real time. In this report, we compare our methods with existing techniques and demonstrate how to resolve instrument response changes in long-period data (>100 seconds) as well as in the microseism bands (5 to 20 seconds).

High quality broadband data recorded by the GSN are fundamental to characterizing a wide range of Earth science issues including: the size and rupture of large earthquakes (*e.g.*, Tsai *et al.* 2005); imaging the interior of the Earth (*e.g.*, Van der Hilst *et al.* 1997); tracking global climate variation (Aster *et al.* 2008); and monitoring calving glaciers (Ekström *et al.* 2003, 2006a).

Recent studies based on theoretical Earth models (Ekström *et al.* 2006b; Davis and Berger 2007) suggest that broadband seismometer gain levels can vary with time. This has also been confirmed, for the STS-1 sensor, experimentally (Yuki and Ishihara 2002). It therefore has become necessary to systematically check for temporal changes in amplitude at GSN stations. Many of these changes are frequency-dependent in nature and not *a priori* predictable (Ekström *et al.* 2006b). Robust methods that can be applied to a large number of stations in a broad range of frequency bands are necessary.

DATA

Seismic data from long-running GSN stations allows for good resolution of a broad range of periods for nearly two decades (Figure 1). For specific data channels discussed throughout this paper, we use the standard for the exchange of earthquake data (SEED) naming convention (Ahern *et al.* 2006). For example, in the case of `IU.ANMO.00.LHZ`, the network code is IU, the station code is ANMO, the location code is 00, and the channel code is LHZ. The network code IU indicates the operator of the network to which the station (ANMO) belongs. The location code 00 refers to a specific sensor, since many GSN stations have multiple instruments. In this case the primary sensor has location code 00 and the secondary sensor has location code 10. Finally, the channel code refers to both the component of motion (*e.g.*, LHN corresponds to north–south motion) and critical recording parameters, such as sample rate. Broadband data (20 or 40 samples per second) have BH channel codes, and long-period data (1 sample per second) have LH channel codes.

Seismic data channels analyzed in this study were selected to test the absolute amplitude variation of specific sensors of interest. By studying both broadband and long-period data channels we are able to resolve both short-period changes in power, often caused by maintenance visits, as well as changes in the long-period characteristics of the sensors, possibly caused by degradation of sensor feedback electronics.

METHODS

Spectral Estimation

We developed two independent tests to monitor period-dependent gain changes at GSN stations. To carry out these tests, we made use of a database of continuous power spectral density (PSD), computed using the PQLX software system (Boaz and McNamara 2008). Data used in this study were obtained from a database of continuous PSDs that is used for quality control and research purposes at Albuquerque Seismological Laboratory (ASL) (McNamara *et al.* 2009). Spectral methods follow the algorithm used to develop the GSN new low and high noise models (NLNM, NHNM; Peterson 1993). PSDs are computed from continuous, overlapping (50%) time series segments (BH channels: one-hour segments sampled at 40 samples per second or 20 samples per second; LH channels: three-hour segments sampled at one sample per second). All available data are included; there is no removal of earthquakes, system transients, or data glitches. The instrument transfer function

doi: 10.1785/gssrl.81.4.605

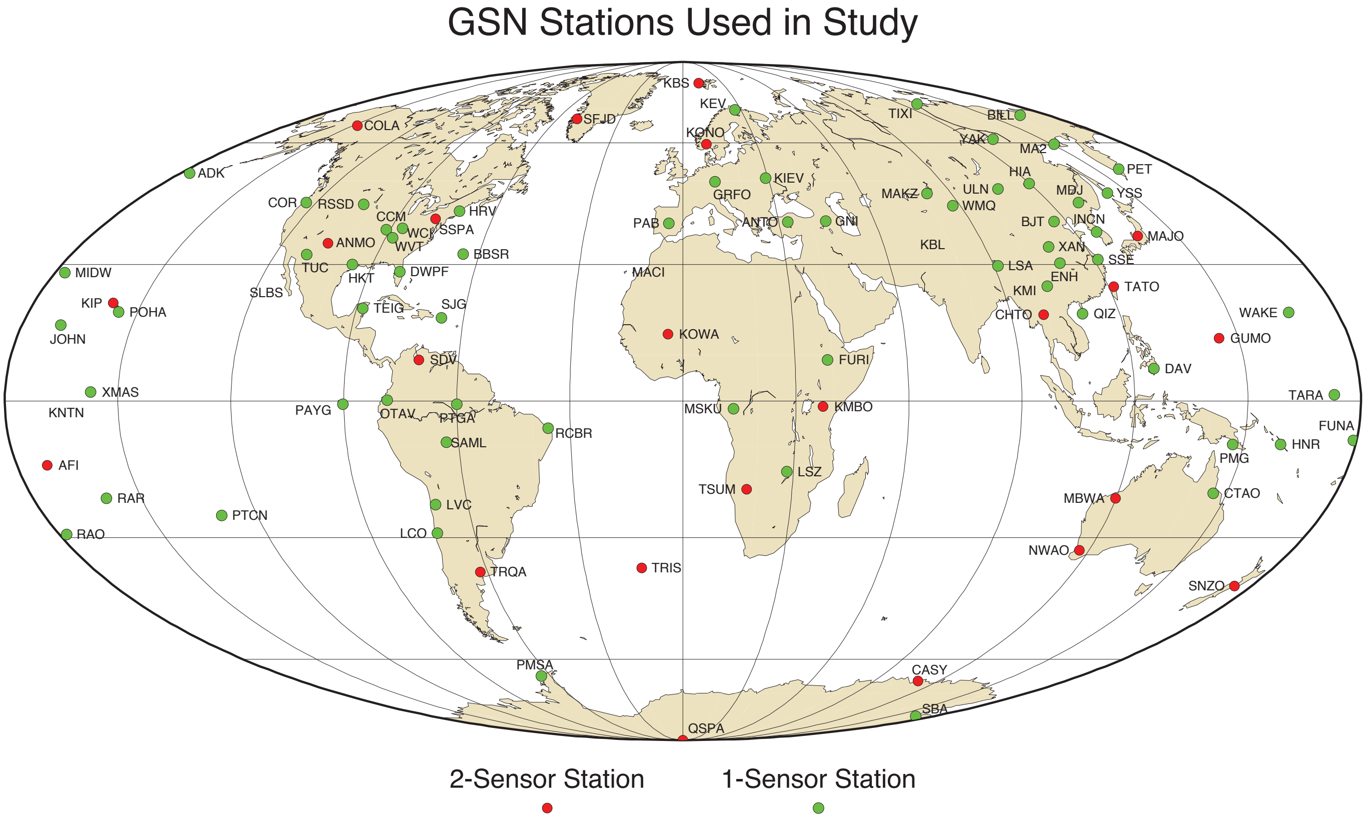

▲ **Figure 1.** GSN map of stations used in the study in our study. Red dots are stations at which both the two-sensor and one-sensor analysis techniques were applied. Green dots correspond to stations where the one-sensor analysis technique was applied. Our list of one-sensor stations includes all IRIS/USGS stations (network code IU) and all IRIS China Digital Seismic Network stations (network code IC).

is deconvolved from each time segment. Each time series segment is divided into 13 subsegments (900 seconds for BH and 2,700 seconds for LH channels), overlapping by 75%. Each subsegment is processed by: 1) removing the mean, 2) removing the long-period trend, 3) tapering using a 10% cosine function, 4) transforming via fast Fourier transform to obtain the amplitude spectrum, and 5) squaring the amplitude spectrum to obtain the power spectrum (McNamara and Buland 2004). Figure 2 shows the nearly 10-year distribution of PSDs for one station used as examples later in this study (IU.KIP; Figure 1), in 1 dB by 1/8 octave bins, gathered into a probability density function (PDF) (after McNamara and Buland 2004). PDFs for all GSN stations analyzed in this study can be found at the ASL ftp site: ftp://aslftp.cr.usgs.gov/pub/users/McNamara/PDFs.

Temporal Change Methods (Multiple Sensors)

We take advantage of the fact that many GSN stations have co-located broadband sensors, which allows for a direct comparison of sensor health. We compared power levels between the vertical components of the two sensors in two microseism period bands (4 to 6 seconds and 18 to 22 seconds) along with a long-period band (90 to 110 seconds) (Figure 2). By focusing on several distinct small-period bands we can decipher between abrupt changes in the power levels, as well as gradual changes in power levels that tend to be visible at longer periods.

For each station in this study with co-located sensors, we compiled daily PDFs for both sensors' vertical components. We then computed a median PSD from the daily PDF distribution and computed band averages of the PDF median over the period bands of interest (4 to 6 seconds, 18 to 22 seconds, or 90 to 110 seconds). By using median power levels we can resolve aggregate changes in power levels and reduce scatter caused by using daily power level values. Figure 3 is an example of daily PDFs and medians for IU.GUMO.00.LHZ and IU.GUMO.10.LHZ (Guam, Mariana Islands) for two different days (20 April 2003 and 13 July 2005). Note the clear change in noise characteristics for IU.GUMO.00.LHZ from 20 April 2003 (Figure 3A) to 13 July 2005 (Figure 3C). We then calculated the difference of the daily band-averaged power levels between the two sensors. We chose daily intervals to remove the effects of large transients due to earthquakes and/or individual sensor and recording system problems.

Figure 4 illustrates the results of the differencing by comparing the power level differences between the KS-54000 seismometer (IU.GUMO.00.LHZ) and the CMG-3T seismometer (IU.GUMO.10.LHZ) (Guam, Mariana Islands) in the 4 to 6 second microseism period band, the 18 to 22 second microseism period band, the 90 to 110 second period band, and also the 90 to 110 second period band after large earthquakes ($M_w > 6.5$). We observe an abrupt 1-dB shift in late 2004 in the 4 to 6 sec-

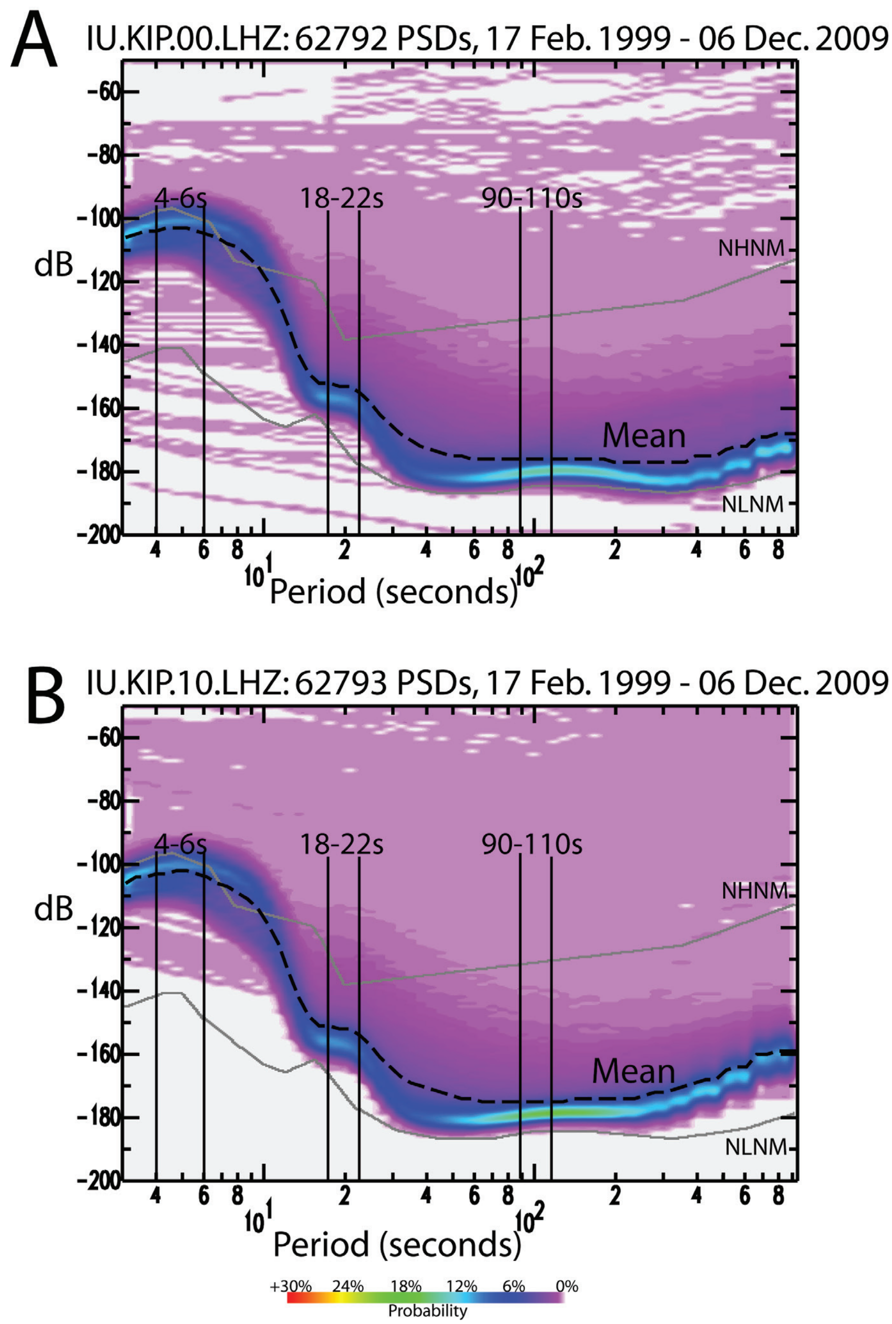

▲ **Figure 2.** Long-term (10-year) PSD PDF examples used in this study. A) PDF for the primary vertical sensor at KIP (IU.KIP.00.LHZ). B) PDF for the secondary vertical sensor at KIP (IU.KIP.10.LHZ). Also shown are the long-term reference means (dashed black lines) and the NHNM and NLNM (solid gray lines) (Petersen 1993).

ond period band that corresponds to a maintenance visit to replace an aging sensor. The 1-dB offset represents an approximately 10% change in power levels between instruments and suggests an error in the instrument response transfer function sensitivity for the new KS-54000 at IU.GUMO.00.LHZ. Although this shift is present in all frequency bands it is difficult to identify because of differences in instrument noise levels between sensors. We found that by using daily medians we were still able to easily identify abrupt changes in instrument characteristics, which might not be easily identified if longer term medians were used. Although there is still considerable scatter when using median power levels, a clear 1-dB offset in the power level is observed toward the end of 2004. The scatter in the differenced data is due to transients, such as spikes and other glitches in the waveform data caused by sensor and/or telemetry problems affecting only one sensor at a station.

Figure 5 shows power level differences between the STS-1 seismometer (IU.AFI.00.LHZ) and the STS-2 seismometer (IU.AFI.10.LHZ, Afiamalu, Samoa). Here, we observe few daily medians showing significant offsets or considerable scatter.

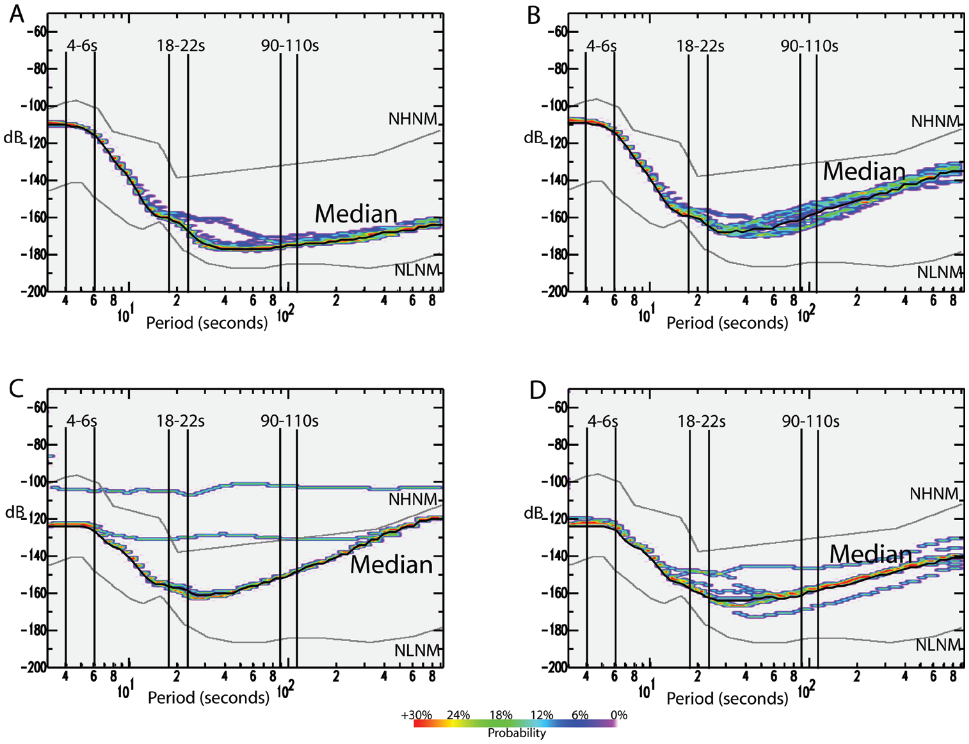

▲ **Figure 3.** Daily PSD PDFs for IU.GUMO demonstrating the daily median method. In all cases the median is denoted by a solid black line. A) PDF on April 20, 2003 for the primary vertical (00.LHZ). B) PDF on April 20, 2003 for the secondary vertical (10.LHZ). C) PDF on July 13, 2005 for the primary vertical (00.LHZ). D) PDF on July 13, 2005 for the secondary vertical (10.LHZ).

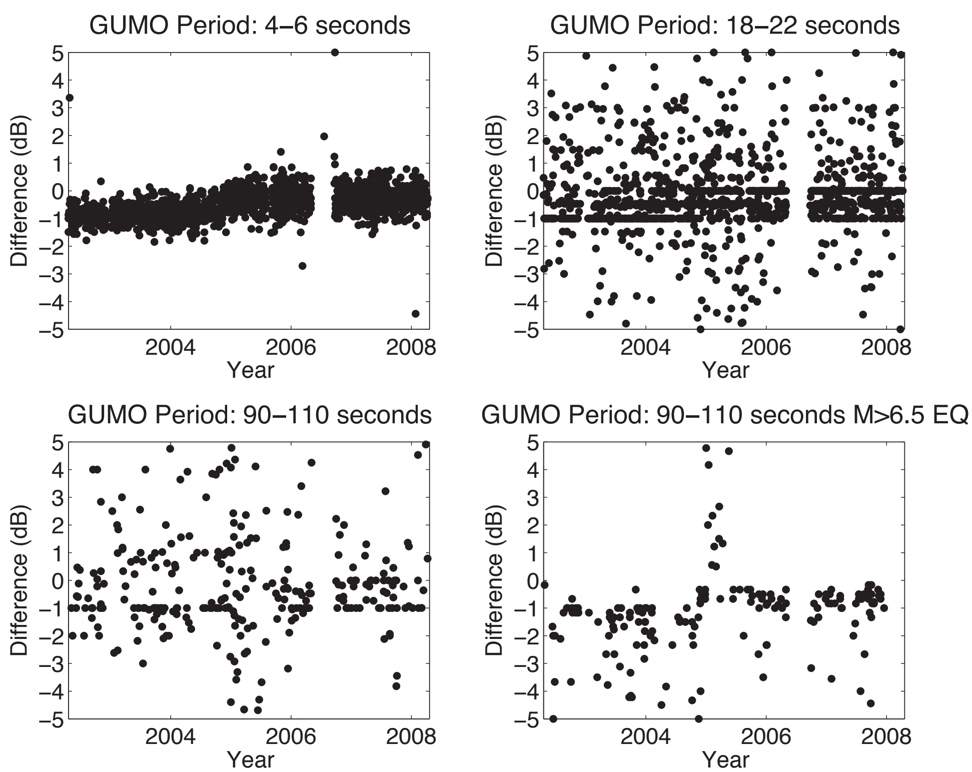

▲ **Figure 4.** Median power level differences between the KS-54000 seismometer (IU.GUMO.00.LHZ) and the CMG-3T seismometer (IU.GUMO.10.LHZ) (Guam, Mariana Islands) in three distinct frequency bands using daily averages as well as after large earthquakes. The 1-dB shift occurring in late 2004 in the 4 to 6 second period difference plot corresponds to a station maintenance visit during which the KS-54000 seismometer was changed out due to a noisy EW component in the previous sensor.

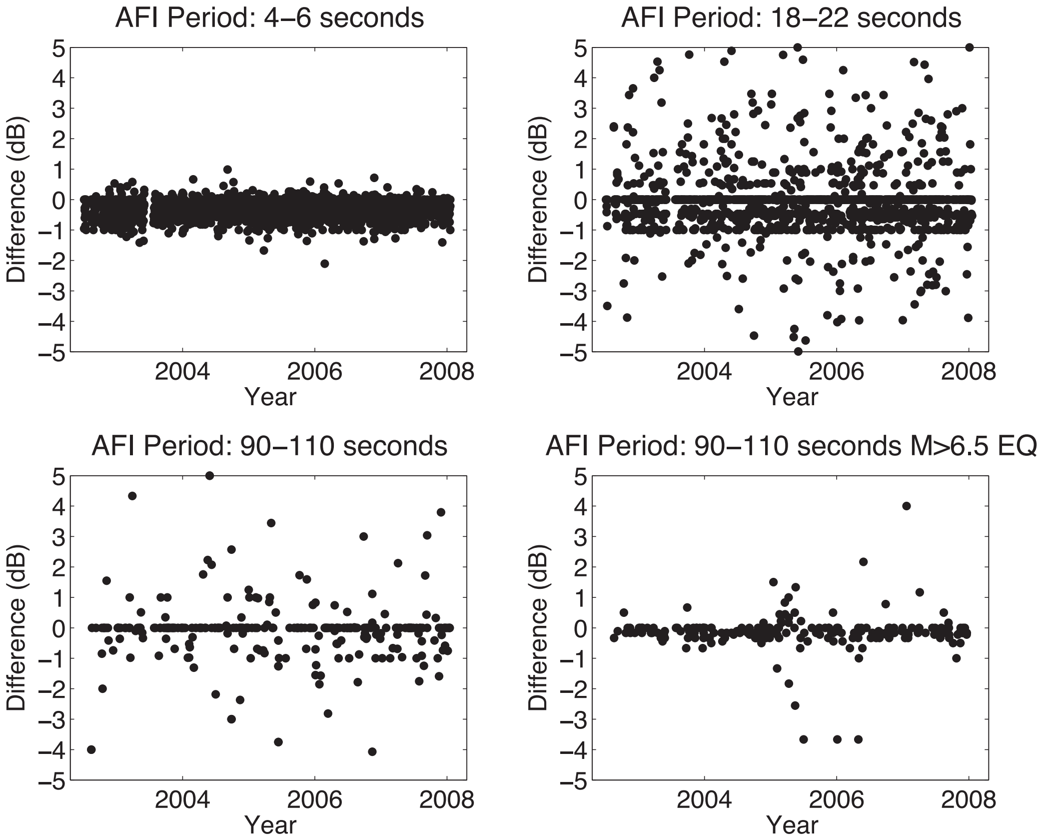

▲ **Figure 5.** Median daily power level differences between the STS-1 seismometer (IU.AFI.00.LHZ) and the STS-2 seismometer (IU.AFI.10.LHZ, Afiamalu, Samoa).

Again, the scatter is likely due to data transients that affect only one sensor at a time.

To further highlight potential frequency-dependent response changes in the long-period band (90 to 110 seconds), we compared median power levels between two vertical components for three-hour time periods after all magnitude $M_w > 6.5$ earthquakes between 1999 and 2008. This approach reduces problems from low signal-to-noise ratio levels. Figure 5 shows power level differences between the STS-1 seismometer (IU.AFI.00.LHZ) and the STS-2 seismometer (IU.AFI.10.LHZ, Afiamalu, Samoa; Figure 1) in the 90 to 110 second band using this method. Here, we observe no consistent offsets in the data, suggesting that there are no significant problems or degradation of the sensors at this station.

Temporal Change Methods (Single Sensor)

As demonstrated above, comparing the power levels between co-located sensors is a useful tool for identifying instrument problems. However, many sites have a single sensor and therefore require a different approach. Moreover, a method that uniquely identifies an errant sensor has broader applicability. To resolve possible temporal gain changes in stations with a single sensor, we compared monthly mean PSDs with total mean PSD power levels from 1999 to 2008. For brevity, we will refer to this method as the "reference mean method" throughout the rest of this paper. This approach also allows us to resolve gain changes in horizontal components without introducing errors caused by orientation differences between co-located sensors.

Using both broadband and long-period channel data, we computed a monthly mean power spectrum along with a long-term "reference" mean power spectrum from 1999 to 2008 for each channel in this study. For each channel we calculated monthly mean power levels and a long-term reference mean power spectrum using data from 1999 to 2008. We then computed differences between the monthly and the long-term power spectra. Figure 2A shows the long-term reference for IU.KIP.00.LHZ. By using means instead of medians we can more effectively resolve changes in power levels. This could be attributed to effectively increasing the resolution by allowing for smaller variations than integer values. We also found that by considering monthly averages instead of daily averages, there was less scatter in power level variations, making it easier to resolve gain changes in a given period band.

Figure 6 shows power level differences between the monthly mean and the reference mean of the STS-1 seismometer (IU.PET.00.LHZ) (Petropavlovsk, Russia) (Figure 1). The alternating red and blue pattern occurring around periods of five seconds corresponds to seasonal variation of the microseism power levels (Aster *et al.* 2008). We observe large variation at the periods of 100 seconds and more that is also clearly observed as a change in the PDF characteristics. The annual elevated power offsets are caused by long-period pulsing. By observing the long-term trends at periods of 100 seconds and

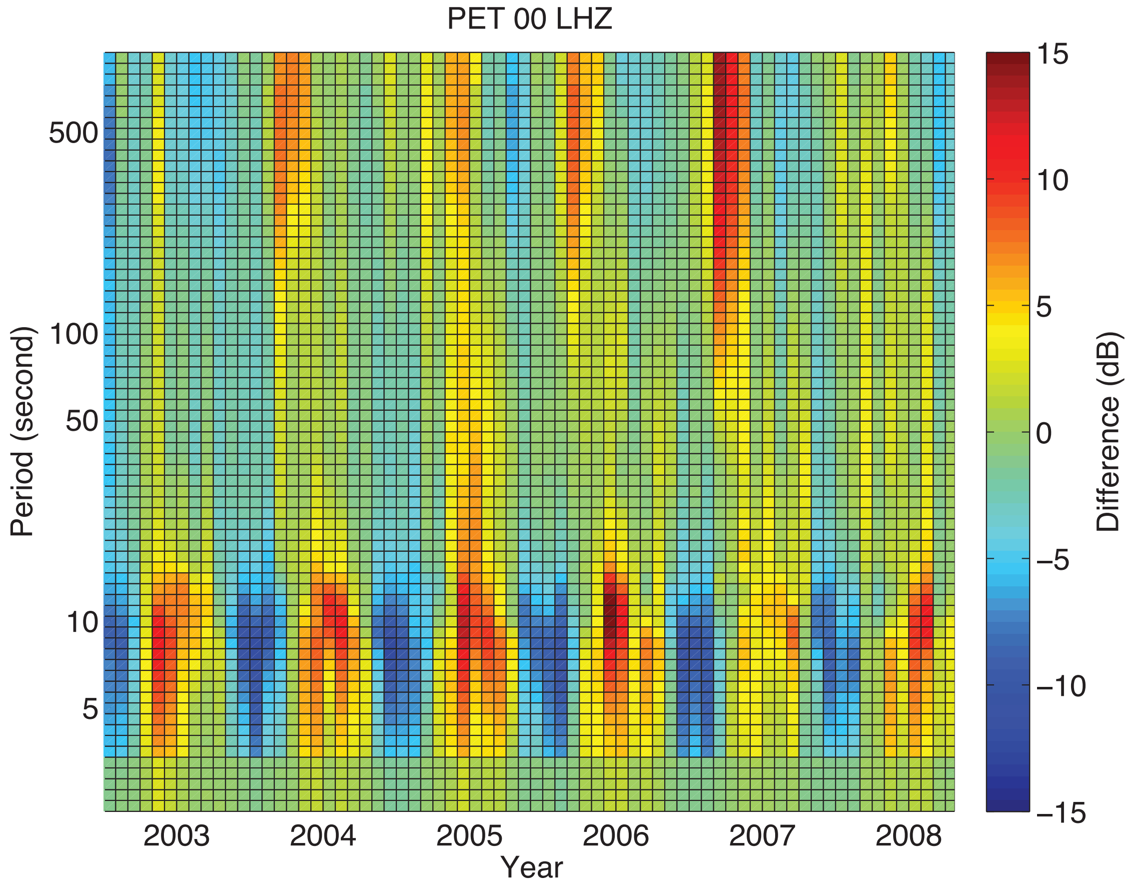

▲ **Figure 6.** Power level differences between the monthly mean and the reference mean for the STS-1 seismometer (IU.PET.00.LHZ, Petropavlovsk, Russia). The power level differences allow us to resolve instrument changes in a large band of frequencies.

more, we see that the instrument's vertical component is slowly developing elevated noise levels. This elevated noise also gives an explanation for why the longer-period pulsing is becoming more apparent, as we are seeing elevated power levels in the long-period band. These observations, for (IU.PET.00.LHZ), are in general agreement with the observations of Davis and Berger (2007) but not easily resolved by the methods of Ekström *et al.* (2006b). A possible explanation for this is that the deviations are amplitude dependent and only seen in the absence of earthquakes or over long time windows.

RESULTS

We applied the above two-sensor daily median analysis to 27 IU GSN stations and the reference mean method to 80 IU GSN stations (shown in Figure 1). In the latter case, we computed temporal mean differences for all components of all sensors and compared with the reference mean for both BH and LH channels. We then compared large observed variations in power level differences with the Incorporated Research Institutions for Seismology (IRIS) data problem report (DPR) records (http://www.iris.edu/data/dpr.htm).

In many cases, changes in power levels correspond to station maintenance visits. For example, using the daily median two-sensor method, we observe a positive 1-dB shift (Figure 7) in the middle of 2000 at IU.KIP (Kipapa, Hawaii) (Figure 1) that was the result of changing a digitizer board in the data acquisition system. A second, negative shift in daily median power levels occurred in the middle of 2005 at IU.KIP and corresponds to a site visit.

Ekström *et al.* (2006b) noted a gradual change in the long-period power levels at IU.KIP during 2004. We observe a similar power level change using the daily median two-sensor method in the 90 to 110 second period band (Figure 7). Significant scatter in our observations obscures the gradual change in the long-period power levels. However, using the daily median differences for time periods after $M_w > 6.5$ earthquakes reduces the scatter significantly and the power level change is more clearly observed (Figure 7). The large earthquake signals improve resolution of this change in response in the 90 to 110 second period range. The gradual decrease in long-period (>500 seconds) power is also well resolved using the reference mean method (Figure 8). The gradual decrease of the power difference in the 100 second and greater period band is truncated by the sharp change in late 2005 that corresponds to the replacement of the STS-1 feedback electronics box. The power level offset decreased after the start of a new epoch on day May 24 (144), 2006. The lack of gradual change in power levels at period bands of less than 90 to 110 seconds indicates a possible change in the instrument's amplitude response. A

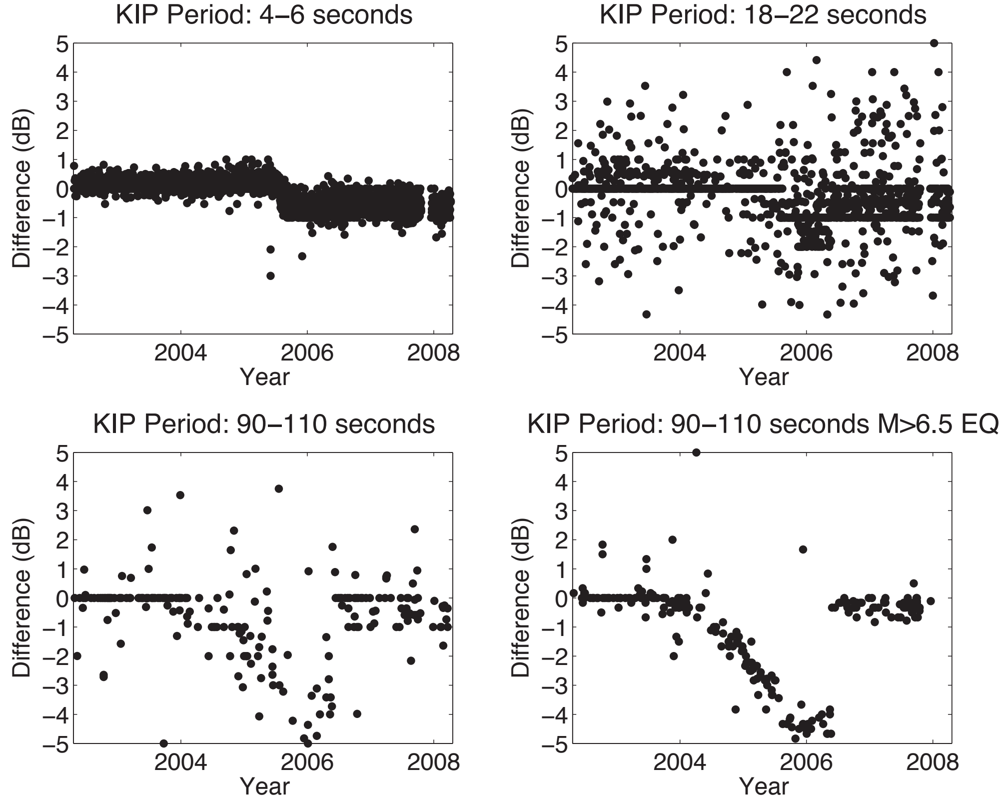

▲ **Figure 7.** Median daily power level differences between the STS-1 seismometer (IU.KIP.00.LHZ) and the STS-2 seismometer (IU.KIP.10.LHZ) (Kipapa, Hawaii). The sharp changes in offset occurring in late 2000 and the middle of 2005 in the 4 to 6 second period band correspond to maintenance visits.

detailed discussion of this phenomenon, along with methods to prevent these decreases in long-period response, was previously discussed by Hutt and Ringler (2009).

DISCUSSION

The methods described in this paper allow us to observe temporal response changes at GSN stations in a broad range of frequencies without relying on Earth models. This provides an independent method to observe changes in the response of long-period broadband instruments. The reference mean method does not rely on Earth models and is useful across a broad band of periods and components of motion. We summarize the benefits of our new method as follows:

1. Good time resolution
2. Independent of Earth models
3. Independent of absolute amplitudes
4. Broadband
5. Can use all components
6. Can be adapted to real-time application
7. Scalable from individual station monitoring to large networks

Moreover, the real-time applicability of our methods has allowed for the development of real-time station health. We are currently monitoring for sensor health, in real time, at a select number of GSN stations using the reference mean methods (Figures 9 and 10). For example, Figure 9 shows a representative daily real-time plot for station IU.ANMO.00. In this figure we have plotted the reference mean in two period bands, for clarity (0.2 to 1 second) and (90 to 110 seconds). We have increased the frequency with which we monitor station power level changes for identifying station problems quickly. We have also plotted the 10th and 90th percentile power-level bands on these plots in order to monitor for long-term changes in station power levels, which can help to identify problems with a sensor. To observe changes in a range of period bands we are also applying the reference mean method, in real time, to four different period bands (0.2 to 1 second, 4 to 6 seconds, 18 to 22 seconds, and 90 to 110 seconds). Eventually we will use these methods to monitor for sensor health at all the GSN stations for which ASL is responsible.

By observing changes in instrument power levels in real time and in different period bands, we will be able to more effectively observe small variations in sensor health. For example, our methods will help to combat the current issues arising from the aging STS-1, whose effects have only been found at periods from 50 to 300 seconds. However, by not restricting ourselves to one period band we are able to identify problems that remain hidden in other regions of the power spectrum. Quick identification of gain changes and other instrument problems will ultimately improve our ability to quickly resolve these problems. Of course, the end result of these efforts will be an improvement in the quality and quantity of GSN seismic data.

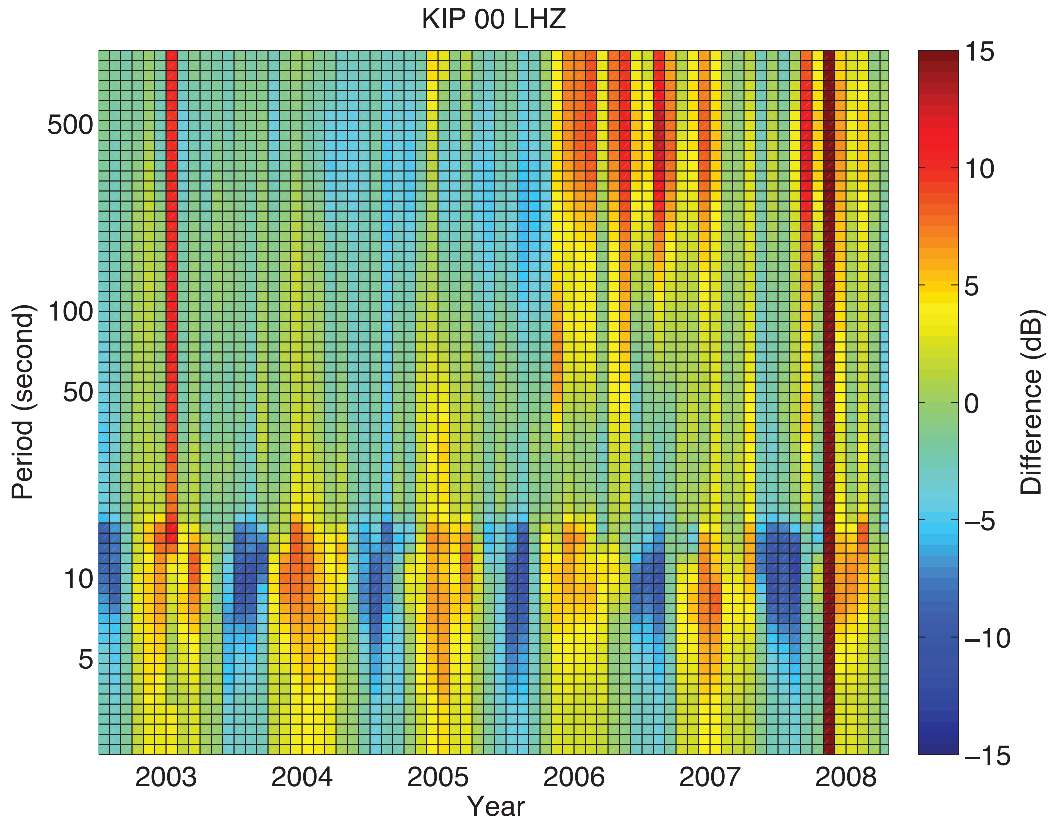

▲ **Figure 8.** Power level differences between the monthly mean and the long-term reference mean for the STS-1 seismometer (IU.KIP.00.LHZ) (Kipapa, Hawaii). The sharp change from blue to red at periods longer than 100 seconds in late 2005 corresponds to when the STS-1 feedback box was replaced.

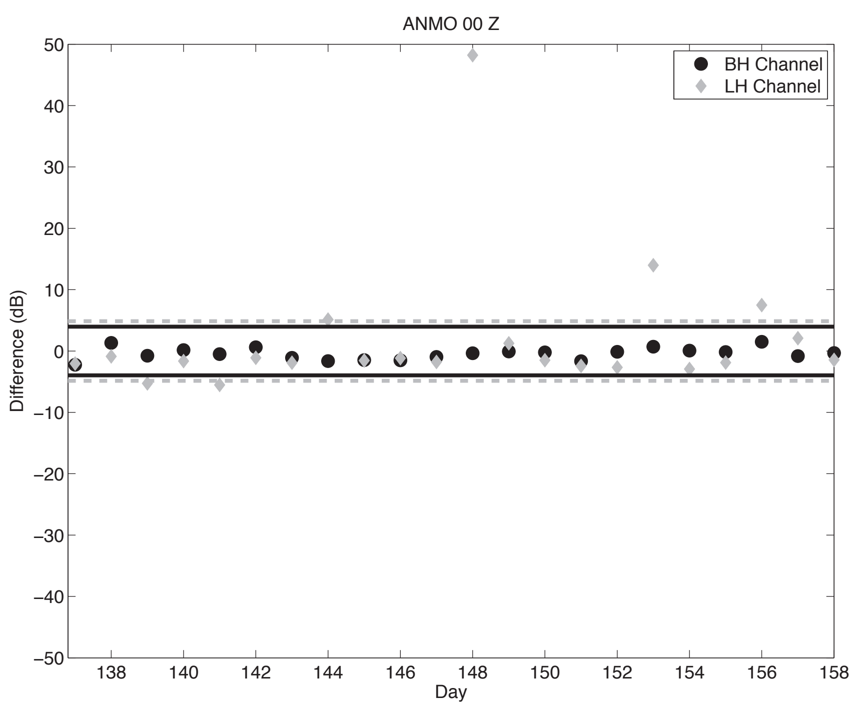

▲ **Figure 9.** Daily power level differences between the daily mean and the reference mean for KS-54000 seismometer (IU.ANMO.00.LHZ) (Albuquerque, New Mexico). The gray dashed line and black solid lines denote the 10th and 90th percentile band for the LH channel 90 to 110 seconds and the BH channel 0.2 to 1 second period bands. The large offset in the long-period difference, on day 148, was the result of an $M_w = 7.1$ earthquake offshore of Honduras.

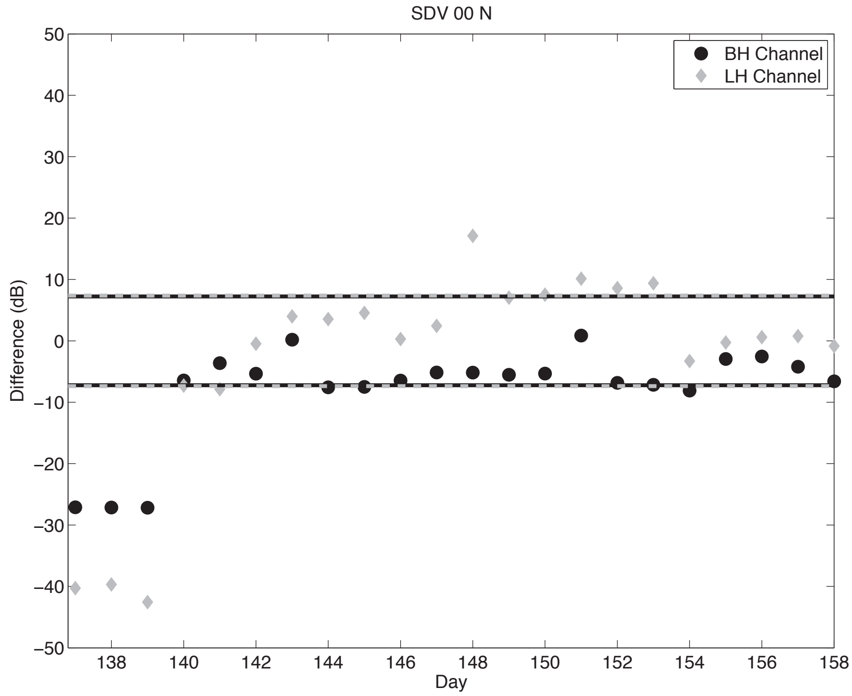

▲ **Figure 10.** Daily power level differences between the daily mean and the reference mean for the STS-1 seismometer at IU.SDV (Santo Domingo, Venezuela), for channel LHN in the period band of 90 to 110 seconds and channel BHN in the period band of 0.2 to one second. The 10th and 90th percentile lines (horizontal lines) for both period bands are within 0.5 dB of each other, making them overlay. The negative power level differences, before day 140, were the result of a blown fuse in the DMA-1 power supply electronics, caused by a power failure.

ACKNOWLEDGMENTS

We would like to thank Cory Gilbert and Tyler Storm, the quality control analysts at ASL, for many useful suggestions. We would also like to thank Eunsil Han for help with plotting our data in real time. Finally, we would like to thank Pete Davis and Tom de la Torre for helpful reviews that improved the presentation of this manuscript. Any use of trade, product, or firm names is for descriptive purposes only and does not imply endorsement by the U.S. Government.

REFERENCES

Ahern, T., R. Casey, D. Barnes, R. Benson, and T. Knight (2007). *SEED Reference Manual*, version 2.4; http://www.iris.washington.edu/manuals/SEEDManual_V2.4.pdf.

Aster, R., D. E. McNamara, and P. Bromirski (2008). Multi-decadal climate-induced variability in microseisms. *Seismological Research Letters* **79**, 194–202.

Boaz, R. I., and D. E. McNamara (2008). PQLX: A data quality control system, uses and applications. *ORFEUS Newsletter* **8** (1).

Davis, P., and J. Berger (2007). Calibration of the global seismographic network using tides. *Seismological Research Letters* **78** (4), 454–459.

Ekström, G., M. Nettles, and G. Abers (2003). Glacial earthquakes. *Science* **302**, 622–624.

Ekström, G., M. Nettles, and V. Tsai (2006a). Seasonality and increasing frequency of Greenland glacial earthquakes. *Science* **311**, 1,756–1,758.

Ekström, G., C. A. Dalton, and M. Nettles (2006b). Observations of time-dependent errors in long-period instrument gain at global seismic stations. *Seismological Research Letters* **77** (1), 12–22.

Hutt, C. R., and A. T. Ringler (2009). Causes and corrections of STS-1 gain changes in the Global Seismographic Network. *Eos, Transactions, American Geophysical Union* **90** (52), fall meeting supplement, Abstract S23A-1735.

McNamara, D. E., and R. P. Buland (2004). Ambient noise levels in the continental United States. *Bulletin of the Seismological Society of America* **94** (4), 1,517–1,527.

McNamara, D. E., C. R. Hutt, L. S. Gee, R. P. Buland, and H. M. Benz (2009). A method to establish seismic noise baselines for automated station assessment. *Seismological Research Letters* **80** (4), 628–637.

Peterson, J. (1993). *Observation and Modeling of Seismic Background Noise*. USGS Technical Report 93-322, 95 pp.

Tsai, V. C., M. Nettles, G. Ekström, and A. M. Dziewonski (2005). Multiple CMT source analysis of the 2004 Sumatra earthquake. *Geophysical Research Letters* **32**, 17. doi:10.1029/2005GL023813.

Van der Hilst, R. D., S. Widiyantoro, and E. R. Engdahl (1997). Evidence for deep mantle circulation from global tomography. *Nature* **386**, 578–584.

Yuki, Y., and Y. Ishihara (2002). Methods for maintaining the performance of STS-1 seismometer. *Frontier Research on Earth Evolution* **2**, 1–5.

U.S. Geological Survey
Albuquerque Seismological Laboratory
P.O. Box 82010
Albuquerque, New Mexico 87198-2010 U.S.A.
aringler@usgs.gov